

[Supplementary Information for]

Atomistic Insights into the Adsorption and Stimuli-Responsive Behavior of Poly(N-isopropylacrylamide)-Graphene Hybrid Systems

Mahdi Moshref-Javadi, George P. Simon, and Nikhil V. Medhekar^{*}

Department of Materials Science and Engineering, Monash University, Clayton, VIC 3800, Australia.

^{*}Corresponding Author: nikhil.medhekar@monash.edu

1- N-Isopropylacrylamide (NIPAM) Monomer:

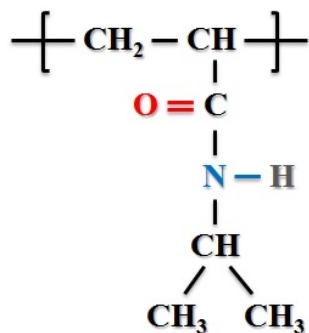


Figure S1. Schematic representation of a monomer of NIPAM.

2- The Applied Force Field:

Investigations on PNIPAM, G and GO in water were studied based on all-atom MD simulations using polymer consistent force-field (PCFF).¹⁻³ This Class II force-field incorporates both covalent and non-covalent terms, and its applicability has been validated by quantum mechanics methods.^{2,4} PCFF has successfully been employed for investigating various polymer systems,⁵ particularly PNIPAM in water and its CG transition^{4,6,7} as well as graphene nanocomposites.⁸⁻¹⁰ Potential energy components of the PCFF force field are as follows:

$$\begin{aligned} E_{\text{total}} = & \sum_{\text{bond } b} [K_2(b - b_0)^2 + K_3(b - b_0)^3 + K_4(b - b_0)^4] \\ & + \sum_{\text{angle } \theta} [H_2(\theta - \theta_0)^2 + H_3(\theta - \theta_0)^3 + H_4(\theta - \theta_0)^4] \\ & + \sum_{\text{torsion } \phi} [V_1[1 - \cos(\phi - \phi_1^0)] + V_2[1 - \cos(2\phi - \phi_2^0)] + V_3[1 - \cos(3\phi - \phi_3^0)]] \\ & + \sum_{\text{out-of-plane } \chi} [k_x \chi^2] \\ & + \sum_{\text{bond } b} \sum_{\text{bond } b'} F_{bb'}(b - b_0)(b' - b'_0) \end{aligned}$$

$$\begin{aligned}
& + \sum_{\text{angle } \theta} \sum_{\text{angle } \theta'} F_{\theta\theta'} (\theta - \theta_0) (\theta' - \theta'_0) \\
& + \sum_{\text{bond } b} \sum_{\text{angle } \theta} F_{b\theta} (b - b_0) (\theta - \theta_0) \\
& + \sum_{\text{bond } b} \sum_{\text{torsion } \phi} (b - b_0) (V_1 \cos \phi + V_2 \cos 2\phi + V_3 \cos 3\phi) \\
& + \sum_{\text{bond } b'} \sum_{\text{torsion } \phi} (b' - b'_0) (V_1 \cos \phi + V_2 \cos 2\phi + V_3 \cos 3\phi) \\
& + \sum_{\text{angle } \theta} \sum_{\text{torsion } \phi} (\theta - \theta_0) (V_1 \cos \phi + V_2 \cos 2\phi + V_3 \cos 3\phi) \\
& + \sum_{\text{torsion } \phi} \sum_{\text{angle } \theta} \sum_{\text{angle } \theta'} F_{\phi\theta\theta'} \cos \phi (\theta - \theta_0) (\theta' - \theta'_0) \\
& + \sum_{i>j} \frac{q_i q_j}{\epsilon r_{ij}} \\
& + \sum_{i>j} \left[\frac{A_{ij}}{r_{ij}^9} - \frac{B_{ij}}{r_{ij}^6} \right] \tag{ES1}
\end{aligned}$$

where b and b' are bond lengths, θ is the bond angle, ϕ is the dihedral torsion angle, χ is the out-of-plane angle, q is the atomic charge, ϵ is the dielectric constant, and r_{ij} is the distance between atom i and atom j . The first four components represent the valence interactions. The next seven components indicate the valence cross-terms, and the last two indicate the Coulombic and van der Waals terms, respectively. The parameters b_0 , K_i ($i = 2-4$), θ_0 , H_i ($i = 2-4$), ϕ_i^0 ($i = 1-3$), V_i ($i = 1-3$), b'_0 , θ'_0 , $F_{bb'}$, $F_{\theta\theta'}$, $F_{b\theta}$, $F_{\phi\theta\theta'}$, A_{ij} and B_{ij} were obtained from the works of Sun *et al.*

1-3

3- Radius of Gyration and Contact Surface Area:

In order to monitor the CG transition, the radius of gyration (R_g) was calculated at each temperature. R_g is a measure of the size of a group of atoms, and is computed using:

$$R_g^2 = \frac{1}{M} \sum_i m_i (r_i - r_{cm})^2 \quad (\text{ES2})$$

where M is the total mass of the polymer chain, r_{cm} is the center-of-mass (COM) of the polymer chain, and the sum is over all the atoms in the polymer chain.

The area of the molecular surface defined by the contact surface between two molecules is called the interface area or contact surface area (CSA) of the molecular assembly. This parameter is an indicative of the adsorption of PNIPAM on the surface, and can be calculated as:¹¹

$$CSA = \frac{1}{2} [(SASA_{PNIPAM} + SASA_{sheet}) - SASA_{complex}] \quad (\text{ES3})$$

where $SASA_{PNIPAM}$ and $SASA_{sheet}$ are the solvent accessible surface areas of the PNIPAM chain and G/GO sheet, respectively, and $SASA_{complex}$ is that of the whole assembly of the sheet and PNIPAM. The solvent accessible surface areas were calculated using the overlapping spheres algorithm.^{12,13}

4- Accuracy of the Computational Model:

The validity of our method and the model was tested by measuring the transition temperature of PNIPAM chain in water using a temperature stepping algorithm. As shown in Figure S2, the polymer did not show any significant change in the R_g value until the temperature reached 304 K, at which it demonstrated a clear decline from ~ 15 Å to ~ 10 Å, followed by a constant R_g with further increase in temperature. This change at 304 K indicates the CG transition, also depicted in Figure S3. The LCST of 304 K is in good agreement with previous simulation and experimental results on PNIPAM CG transition,^{14,15} and illustrates the validity of the applied method.

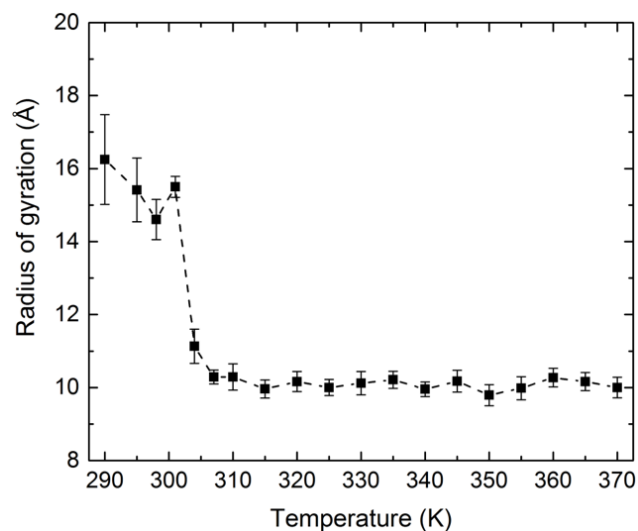


Figure S2. CG transformation of PNIPAM in water at 304 K as revealed by the decrease in R_g . For visualization snapshots, see Figure S3.

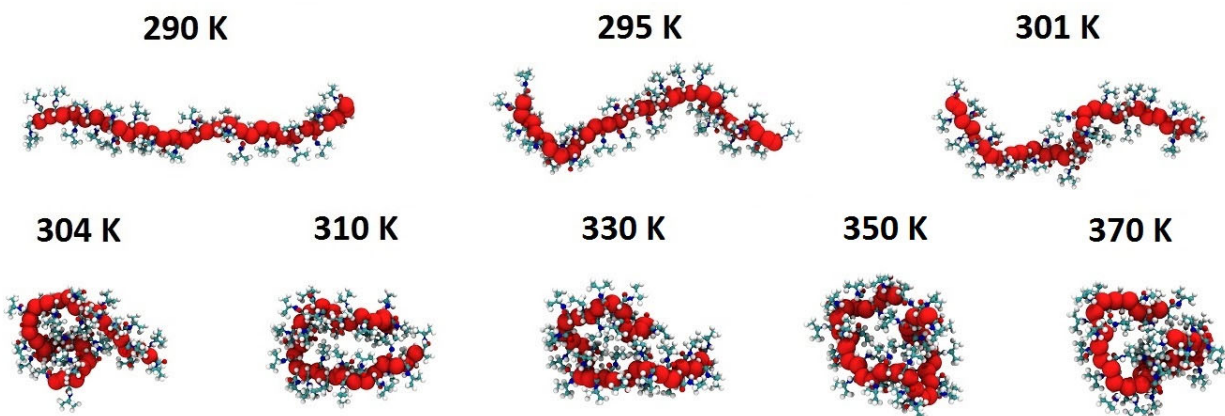


Figure S3. Representative snapshots for PNIPAM in water at various temperatures. Water molecules are not shown for clarity.

5- Simulated Annealing:

To examine the temperature stepping method adequately samples the configurational phase space, we performed simulated annealing at high temperatures followed by a slow cooling for two representative cases of PNIPAM conformations on G (Figure S4) and two representative cases of PNIPAM conformations on GO (Figure S5). Here, the system was heated to 1000 K, followed by cooling via temperature down-stepping. Finally, the samples were annealed at

temperatures below and above the LCST of PNIPAM (Figures S4a and S5a). For PNIPAM-G, the two final temperatures were 330 K and 370 K, while for PNIPAM-GO, temperatures were 298 K and 310 K. Figure S4b and S5b show the evolution of the values of R_g , while Figures S4c,d and S5c,d show the fully equilibrated configurations at the corresponding temperatures. In PNIPAM-G system, the values for R_g were $R_{g(330\text{ K})} = 17.5 \pm 0.4 \text{ \AA}$ (coil) and $R_{g(370\text{ K})} = 12.7 \pm 0.2 \text{ \AA}$ (Globule), whilst in PNIPAM-GO system, they were $R_{g(298\text{ K})} = 16.2 \pm 0.6 \text{ \AA}$ (coil) and $R_{g(310\text{ K})} = 11.0 \pm 0.2 \text{ \AA}$ (Globule). Overall, these results are fully consistent with those obtained from the temperature stepping algorithm, thus confirming an effective sampling of the phase space.

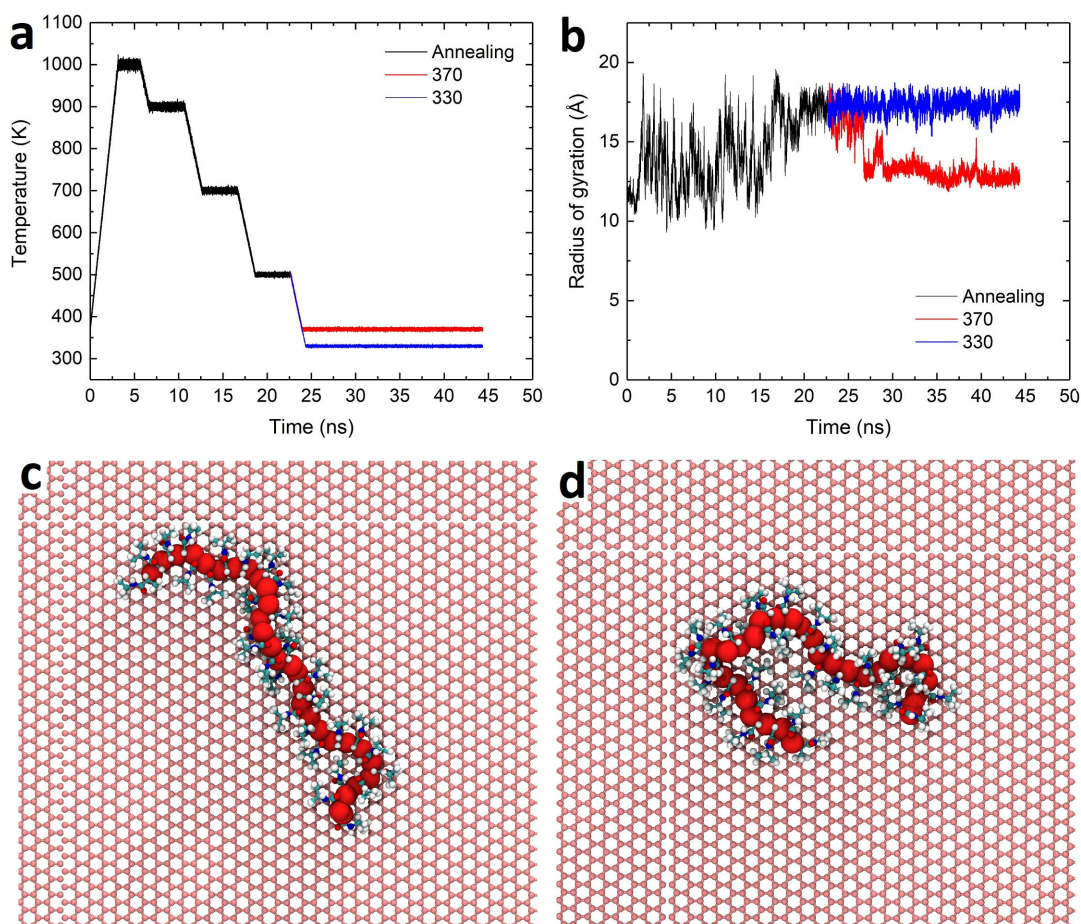


Figure S4. Method and results of the simulated annealing for PNIPAM-G system: (a) Simulated annealing algorithm, and (b) evolution of R_g as a function of time. Representative snapshots for the configuration of PNIPAM on G at 330 K (c), and 370 K (d). Carbon atoms of the polymer backbone are shown by red spheres. Water molecules are not shown for clarity.

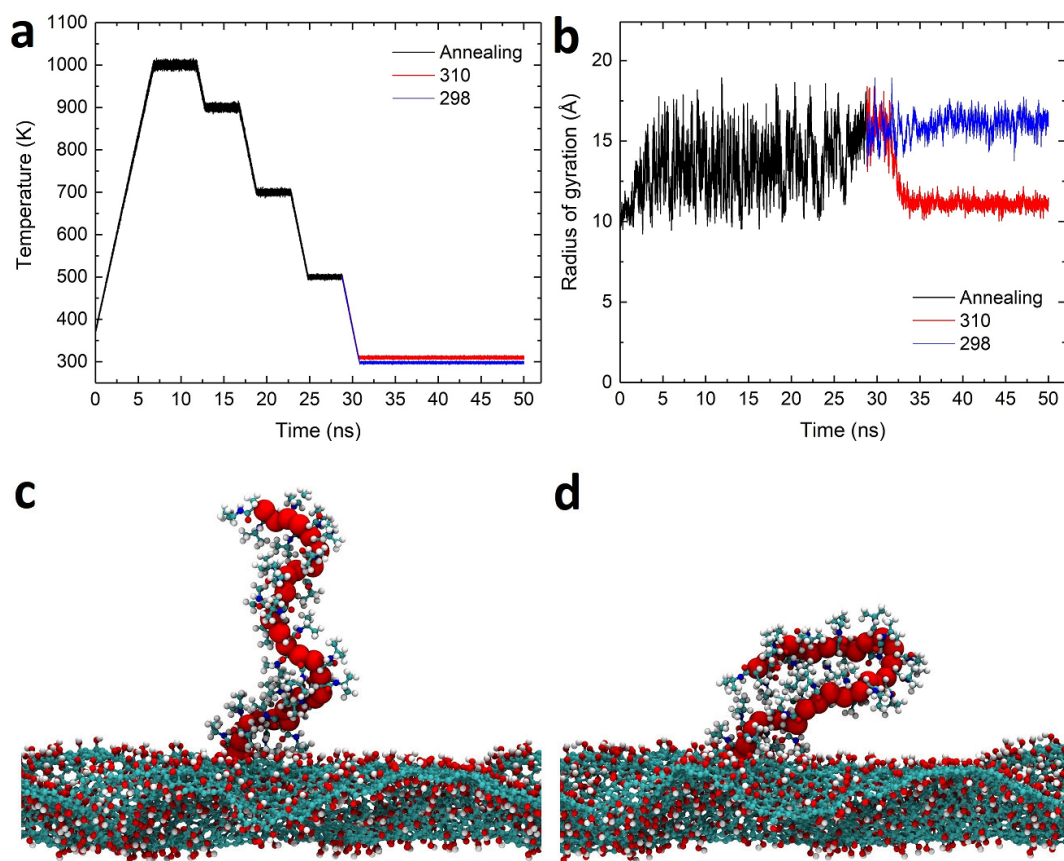


Figure S5. Method and results of the simulated annealing for PNIPAM-GO system: (a) Simulated annealing algorithm, and (b) evolution of R_g as a function of time. Representative snapshots for the configuration of PNIPAM on GO at 298 K (c), and 310 K (d). Carbon atoms of the polymer backbone are shown by red spheres. Water molecules are not shown for clarity.

6- Radial Distribution Functions:

Radial distribution functions (RDF) were calculated for major atoms of PNIPAM with respect to the oxygen atoms of water molecules to examine the arrangement of water molecules in the proximity of PNIPAM (Figure S6). The curves in the RDF diagrams correspond to PNIPAM before and after the CG transition. RDF curves for O_p-O_w and $C_{h2b}-O_w$ in hybrid systems resemble those of a single PNIPAM chain in water. The curves also show peak shifts and reduced peak intensities as a result of a transition to the globular form, indicating that fewer water molecules surround PNIPAM in the globular configuration. Given that the first two peaks

correspond to the first two hydration layers, it can be seen that the second peaks in $C_{h2b}-O_w$ curves are still maintained in the adsorbed state, demonstrating that adsorption of PNIPAM onto G/GO in the coil form does not distort the proximal second hydration layer.⁶ The globular PNIPAM on G/GO leads to a distortion of the second hydration layer, as indicated by the significantly reduced intensity of the second peak in the RDF curves of the $C_{h2b}-O_w$ pair. These observations again substantiate the formation of the globular configuration for the adsorbed PNIPAM.

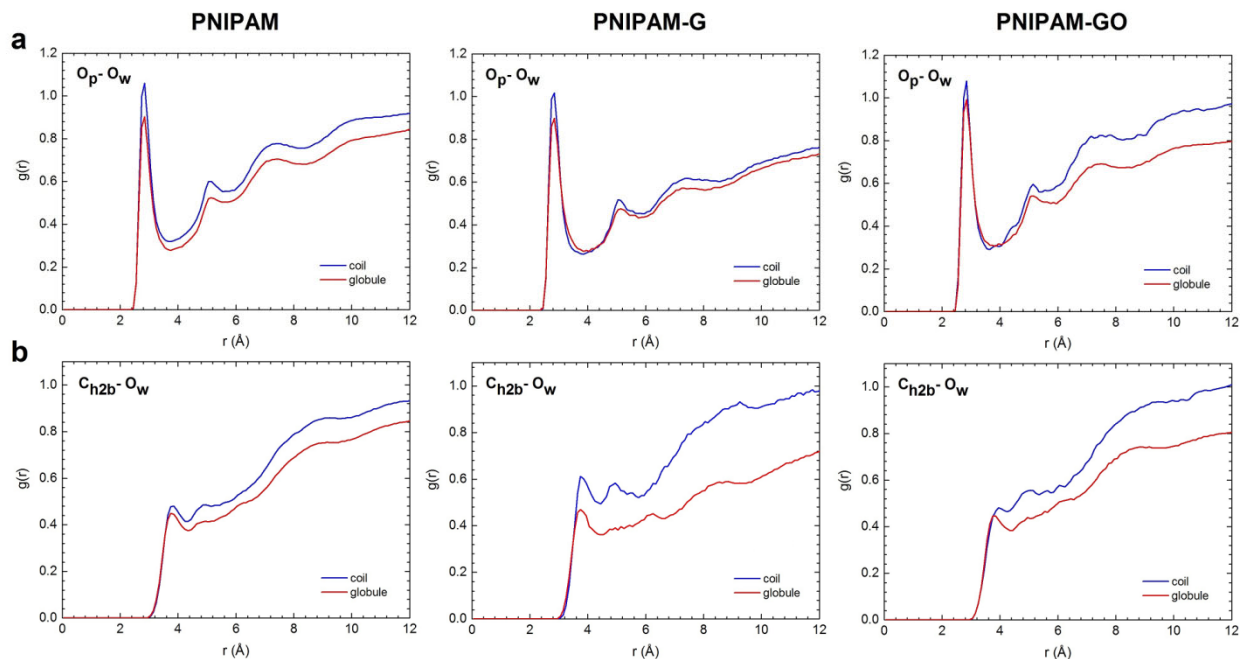


Figure S6. RDF diagrams for (a) O_p-O_w and (b) $C_{h2b}-O_w$ pairs in PNIPAM, PNIPAM-G, and PNIPAM-GO systems. O_p , O_w , C_{h2b} represent oxygen atom of PNIPAM, oxygen atom of water molecule, and carbon atom of $-CH_2$ group in PNIPAM backbone, respectively.

7- Hydrogen Bonding:

Intermolecular and intramolecular hydrogen bonds were investigated to further study the hydrophilic interactions and solvation of the polymer chain. Possible sites for the formation of hydrogen bonds in PNIPAM are carbonyl oxygen (O_p) and hydrogen of amide group (H_p). In GO, potential sites for hydrogen bonding are oxygen of epoxy groups (O_{GO}) and hydrogen (H_{GO})

and oxygen (O_{GO}) of hydroxyl groups, while in a water molecule bonding can form via hydrogen (H_w) and water oxygen (O_w).

As shown in Figure S7a, the pure polymer formed on average 62 hydrogen bonds with water molecules in the first hydration layer. This value decreased to a mean value of 48 at 304 K, with no substantial change upon increasing the temperature to 370 K. This decline indicates the CG transition, which results in fewer hydrogen bonds between PNIPAM and water molecules, but more intramolecular hydrogen bonds in PNIPAM (Figure S7a). Similar results were reported by Abbott *et al.*¹⁶ The reduced number of hydrogen bonds between polymer and water molecules indicates its less hydrophilic nature at high temperatures and is consistent with the decreased number of water molecules in the first hydration layer. This finding again confirms that polymer-water hydrogen bonds play a crucial role in keeping the polymer in an extended form.

For PNIPAM adsorbed on G sheets, the average number of hydrogen bonds between PNIPAM and water molecules decreased from 51 to 47 at 350 K (Figure S7b), associated with the CG transition. The former value, which corresponds to the coil configuration of PNIPAM, was greater compared with that of an individual globular PNIPAM molecule (Figure S7a). This indicates that the adsorption on G occurred mostly via hydrophobic groups, whereby the hydrophilic segments still had the opportunity to form hydrogen bonds, thus retaining their hydrophilic characteristic.¹⁷⁻¹⁹ Additionally, the number of intramolecular hydrogen bonds in PNIPAM shows an increase at 350 K due to the CG transition. The intramolecular hydrogen bonds were preserved with further increase in temperature which corroborates formation of a tightly collapsed-chain conformation and confirms the occurrence of the CG transition in the hybrid system.²⁰

Figure S7c illustrates the number of hydrogen bonds for PNIPAM adsorbed on GO sheet as a function of temperature. The transformation at 304 K was accompanied by a decrease in the number of PNIPAM–water intermolecular hydrogen bonds from 55 to 47, while the number of intramolecular hydrogen bonds increased. As with PNIPAM on G, this increase in intramolecular hydrogen bonds is minor compared to the intermolecular hydrogen bonds formed with water molecules. In contrast to the PNIPAM adsorbed on G, PNIPAM can form intermolecular hydrogen bonds with GO. Although few of these bonds were formed, they were retained with further increase of temperature and through the CG transition.

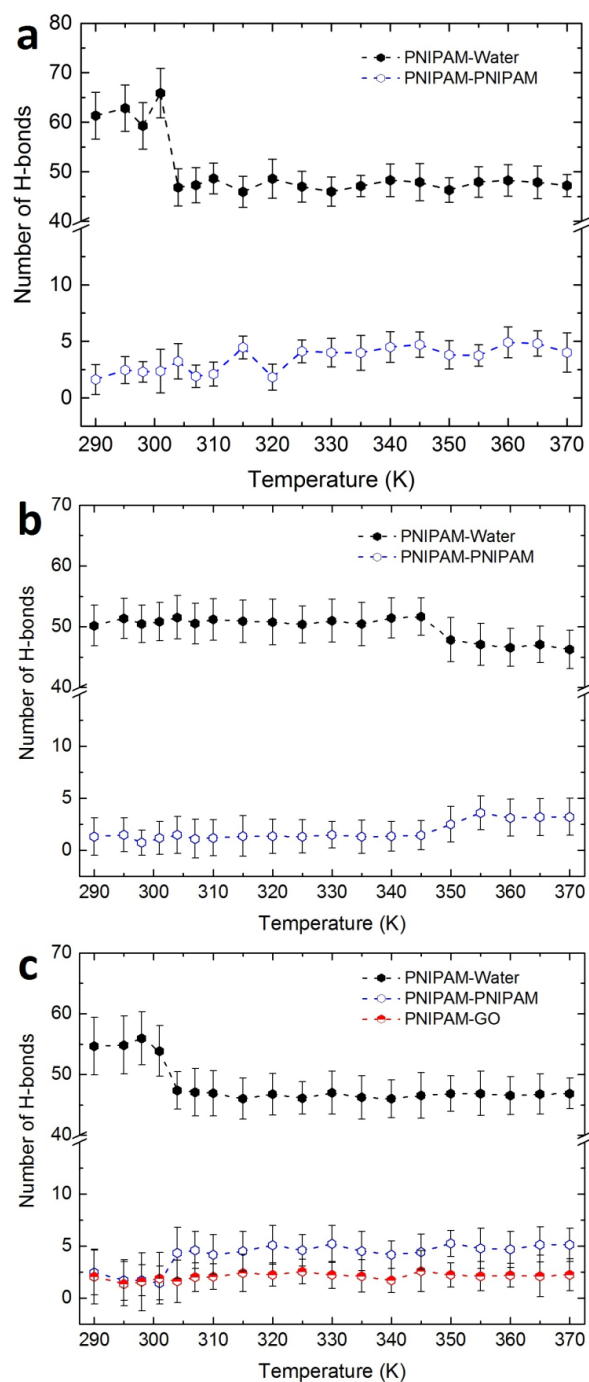


Figure S7. Variations of the number of hydrogen bonds between various components in (a) PNIPAM, (b) PNIPAM-G, and (c) PNIPAM-GO in aqueous solution and at various temperatures.

8- Conceptual Explanation for the LCST Change of PNIPAM in Hybrid Systems:

Fundamentally, the CG transition of PNIPAM is driven by entropy increase, largely due to an increase in the configurational freedom of the water molecules formerly H-bonded with the polymer. When polymer is strongly adsorbed on the G surface, it releases fewer water molecules from its first hydration layer during the CG transition as compared with the transformation of a pure PNIPAM. This is represented as a smaller line slope for the adsorbed polymer in globule form compared to the line for a pure globule PNIPAM ($\alpha_1 > \alpha_2$) (Figure S8). Overall, this results in an increase in the LCST of PNIPAM adsorbed on the surface of G.

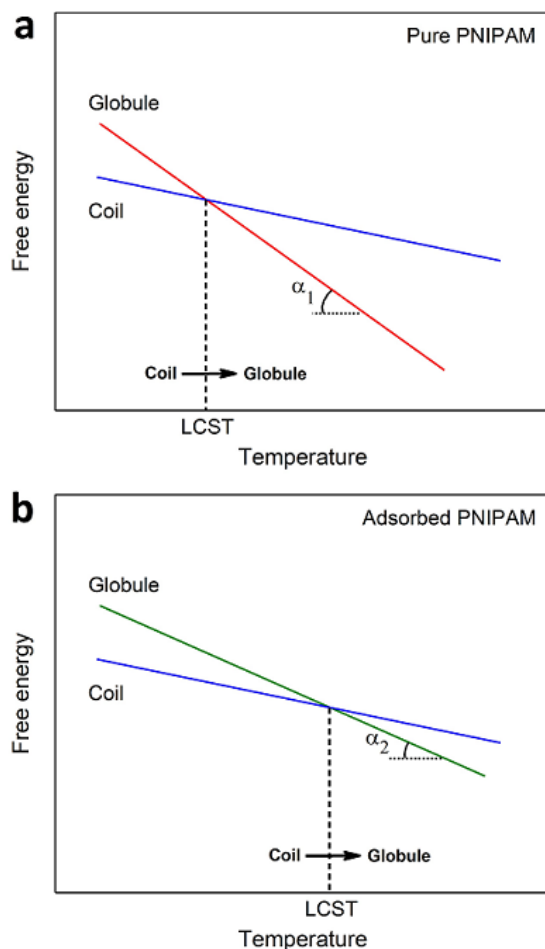


Figure S8. A schematic illustration of the thermodynamics of phase stability of PNIPAM in aqueous solution. (a) Pure PNIPAM, the CG transition occurs at the conventional LCST (~304 K). (b) Adsorbed PNIPAM, the CG transition occurs at higher temperatures. Adsorption on the surface causes a smaller increase in entropy during the formation of the globule phase ($\alpha_1 > \alpha_2$), leading to an increased LCST.

References

- (1) Sun, H. Force field for computation of conformational energies, structures, and vibrational frequencies of aromatic polyesters. *J. Comput. Chem.* **1994**, 15, 752-768.
- (2) Sun, H.; Mumby, S. J.; Maple, J. R.; Hagler, A. T. An ab initio CFF93 all-atom force field for polycarbonates. *J. Am. Chem. Soc.* **1994**, 116, 2978-2987.
- (3) Sun, H.; Mumby, S.; Maple, J.; Hagler, A. Ab initio calculations on small molecule analogs of polycarbonates. *J. Phys. Chem.* **1995**, 99, 5873-5882.
- (4) Pang, J.; Yang, H.; Ma, J.; Cheng, R. Solvation behaviors of N-isopropylacrylamide in water/methanol mixtures revealed by molecular dynamics simulations. *J. Phys. Chem. B* **2010**, 114, 8652-8658.
- (5) Deshmukh, S. A.; Li, Z.; Kamath, G.; Suthar, K. J.; Sankaranarayanan, S. K.; Mancini, D. C. Atomistic insights into solvation dynamics and conformational transformation in thermo-sensitive and non-thermo-sensitive oligomers. *Polymer* **2013**, 54, 210-222.
- (6) Deshmukh, S. A.; Sankaranarayanan, S. K.; Suthar, K.; Mancini, D. C. Role of solvation dynamics and local ordering of water in inducing conformational transitions in poly (N-isopropylacrylamide) oligomers through the LCST. *J. Phys. Chem. B* **2012**, 116, 2651-2663.
- (7) Deshmukh, S. A.; Sankaranarayanan, S. K.; Mancini, D. C. Vibrational spectra of proximal water in a thermo-sensitive polymer undergoing conformational transition across the lower critical solution temperature. *J. Phys. Chem. B* **2012**, 116, 5501-5515.
- (8) Rahman, R.; Haque, A. Molecular dynamic simulation of graphene reinforced nanocomposites for evaluating elastic constants. *Procedia Eng.* **2013**, 56, 789-794.
- (9) Rahman, R. The role of graphene in enhancing the stiffness of polymeric material: A molecular modeling approach. *J. Appl. Phys.* **2013**, 113, 243503.
- (10) Liu, F.; Hu, N.; Ning, H.; Liu, Y.; Li, Y.; Wu, L. Molecular dynamics simulation on interfacial mechanical properties of polymer nanocomposites with wrinkled graphene. *Comput. Mater. Sci.* **2015**, 108, 160-167.
- (11) Balamurugan, K.; Singam, E. A.; Subramanian, V. Effect of curvature on the α -helix breaking tendency of carbon based nanomaterials. *J. Phys. Chem. C* **2011**, 115, 8886-8892.
- (12) Shrake, A.; Rupley, J. Environment and exposure to solvent of protein atoms. Lysozyme and insulin. *J. Mol. Biol.* **1973**, 79, 351-371.
- (13) Durham, E.; Dorr, B.; Woetzel, N.; Staritzbichler, R.; Meiler, J. Solvent accessible surface area approximations for rapid and accurate protein structure prediction. *J. Mol. Model.* **2009**, 15, 1093-1108.
- (14) Tucker, A. K.; Stevens, M. J. Study of the polymer length dependence of the single chain transition temperature in syndiotactic poly (N-isopropylacrylamide) oligomers in water. *Macromolecules* **2012**, 45, 6697-6703.
- (15) Wu, C.; Wang, X. Globule-to-coil transition of a single homopolymer chain in solution. *Phys. Rev. Lett.* **1998**, 80, 4092.
- (16) Abbott, L. J.; Tucker, A. K.; Stevens, M. J. Single Chain Structure of a Poly (N-isopropylacrylamide) Surfactant in Water. *J. Phys. Chem. B* **2015**, 119, 3837-3845.
- (17) Lee, D. Y.; Yoon, S.; Oh, Y. J.; Park, S. Y.; In, I. Thermo-Responsive Assembly of Chemically Reduced Graphene and Poly (N-isopropylacrylamide). *Macromol. Chem. Phys.* **2011**, 212, 336-341.
- (18) Kim, M. J.; Kim, D. W.; Yun, J. S.; Lee, D. H.; Oh, Y. J.; Nam, J. A.; Kim, S. R.; Lee, J. H.; Park, S. Y.; Min, B.-G. Preparation of stable dispersions of chemically reduced graphene oxide through noncovalent interactions with poly (N-isopropyl acrylamide)-grafted pluronic copolymer. *J. Mater. Sci.* **2013**, 48, 3357-3362.
- (19) Dong, J.; Weng, J.; Dai, L. The effect of graphene on the lower critical solution temperature of poly (N-isopropylacrylamide). *Carbon* **2013**, 52, 326-336.
- (20) Kang, Y.; Joo, H.; Kim, J.S., Collapse–Swelling Transitions of a Thermoresponsive, Single Poly (N-isopropylacrylamide) Chain in Water. *J. Phys. Chem. B* **2016**, 120, 13184-13192.